Autonomous gas detection and mapping with unmanned aerial vehicles

Maurizio Rossi *Student Member* and Davide Brunelli *Member*

***Abstract*—Unmanned aerial vehicles (UAVs) are nowadays largely employed in civil applications. One of the most promising is the environmental monitoring (or risk assessment). We propose a battery-powered eNose board that can be embedded with any kind of drones. We evaluated the effectiveness of the sensing method by means of field experiments using the prototype as payload of a hexacopter. Results show that the analysis of the target environmental parameters is not perturbed by the air flow generated by propellers. The system is suitable for any kind of mobile of carrier (UAVs or wheeled robots) thanks to its light weight and compact form factor. To further extend the limited flight autonomy of the carrier we developed an optimal monitoring algorithm for gas leakage localization, a simulating framework to evaluate its performance and we provide a design space exploration for solar powered drones.**

***Index Terms*—Gas leakage localization, Volatile chemicals mapping, Low-power electronics, Embedded gas sensing system, Unmanned aerial vehicles.**

I. Introduction

UNMANNED Aerial Vehicles or drones are nowadays very popular and widely used in scientific research for distributed data collection and remote sensing. A mobile robot equipped with embedded systems can collect environmental samples with a much denser spatio-temporal resolution than a human operator resulting also in an safer working condition.

Pollution and urban air quality are majors environmental risks to public health. Gas emissions are responsible for a variety of respiratory illnesses and environmental problems, such as acid rain and the depletion of the ozone layer. Pollutants may be released as exhaust gases from traffic or industry and fires or as a consequence of accidents with chemicals. Most of volatile compounds are colourless, tasteless and odourless hence, human beings are not able to recognize these leakages early enough to activate appropriate counter measures without auxiliary tools. Moreover, seeking refuge into areas assumed to be non-dangerous because of the missing smell is obviously prone to fatal accidents. The increasingly strict regulation in this regard, requires technological improvements to avoid high concentration in the air to keep a clean environment, to avoid any risks for people and goods and ensure safety in industrial & public environments.

Currently, many monitoring systems consist of a static network of sensors which are distributed at key locations but, in order to obtain a truthful representation of the gas distribution and be able to locate gas sources, it is essential to collect spatially distributed concentration measurements. However, the response of low-cost, chemoresistive gas sensors is caused by direct interaction of the chemical compounds with the sensor surface (1 cm^2), and thus represents a volume (few dm^3) around the sensor surface. Hence, for economical and deployment-related reasons, a stationary sensor network is not a viable solution in many cases. Vehicles can make a significant contribution in this area providing versatile systems for autonomous monitoring of diverse environments.

In this work, we present an embedded electronic platform able to instrument any kind of drone with a chemical sensing system for environmental monitoring, gas leakage detection and pollution mapping applications. We developed a lightweight electronic system, based on a 32MHz/32bit wireless microcontroller unit (MCU) that manages a GSM/GPS modem, a digitally controlled analog interface to drive MOX gas sensors and a micro SD-card for local logging. The two wireless interfaces, a short range 2.4GHz radio based on the IEEE 802.15.4 standard and the GSM/GPRS one, allow the development of custom and smart applications for real-time data sharing and/or alarm notification. The complete 16 cm^2 board (4x4 cm) is battery powered (Li-ion 1800 mAh) and the total weight is less than 30 gr. The remarkably low weight allows the choice of any kind of carrier, not only UAVs, but also wheeled robots, public transportation means and so on, taking advantage of their tour to create real-time mapping of the urban air quality.

The most important design parameter is the energy autonomy of the drone for gas leakage localization and mapping which deals with weight of the system (the payload) and electrical power consumption. No commercial drones exists with autonomy longer than one hour and MOX gas sensors, like GSM modems, consume a remarkable amount of power. Differently from other works in the field we focused on increasing the energy autonomy of the whole platform, carrier and sensing system. For this reason we present the design of the modular embedded sensing system on top of which we developed and simulated a novel algorithm that exploits adaptive sampling to locate the gas leakage minimizing the energy required by the sensing element. We conducted a set of simulations to evaluate the optimal tradeoff between speed of the carrier, energy consumption and gas localization capability. Finally, we present a design space exploration to evaluate the impact of introducing solar panels on top of commercially available drones. As a result we were able to determine the trade-offs among UAV size, payload capacity, energy consumption, solar panel size and expected autonomy

Authors are with the Department of Industrial Engineering, University of Trento, via Sommarive, 9, Trento, 38123, Italy, Phone: (0039) 0461-285350, email: {name.surname}@unitn.it

The work presented in this paper was supported by the project GreenDataNet (grant n.609000), funded by the EU 7th Framework Programme.

This article is an extended version of the paper published in the Proceedins of the IEEE Sensors Applications Symposium 2015 [1].

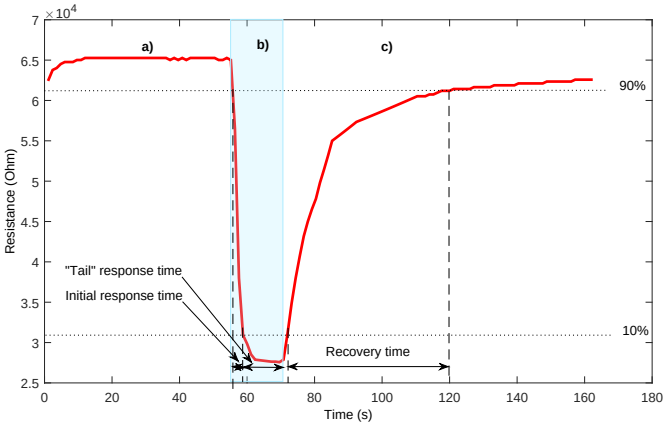

Fig. 1. Characteristic response of continuously powered MOX sensors.

gain.

II. Related Works

UAVs or drones, have overcome their first military uses, becoming today one of the most important technologies in data collection and remote sensing [2]. This is highlighted by several researches, which list among its advantages a high resolution and positional accuracy. Their relevance for Earth system understanding and environmental science research has been pointed out for example in [3]. Among the others, localization and mapping of geographical areas by means of advanced 3D imaging techniques have been demonstrated [4], [5]. Its uses for civil purposes include various applications of gas detection, such as obtaining gas distribution mapping, monitoring emissions and gas source localization in geographical areas where environmental concern is a hot topic [6]–[9]. They have also been investigated for emergency handling in indoor environments [10]. The main problems of all the current implementation are (i) the limited flight autonomy and (ii) the size-to-payload ratio; few efforts have been dedicated so far to the joint optimization of the flight path and energy consumption of chemical sensors.

Currently, some research teams have demonstrated solar power UAVs for remote sensing and wide-area monitoring applications [11] to solve the problem of the limited flight-autonomy; as far as we know those systems are based on airplane-like drones that offers big surfaces (wings and fuselage) to host photovoltaic (PV) panels but precise positioning and hoovering can not be achieved with these devices. Following this research trend we propose an analysis on the expected performance boost of employing PV panels on multi-rotor copters against the power-to-payload ratio, considering numbers from commercial drones' manufacturers.

On the volatile chemical sensing side, also known as eNose applications [12], [13], three main technologies exist that are suitable for distributed monitoring using autonomous equipment, that require compactness, low-weight and low-power characteristics: chemo-optical [14], chemoresistive [15], [16] and electrochemical [17]. Chemo-optical devices are the most expensive and bulky while electrochemical sensors need

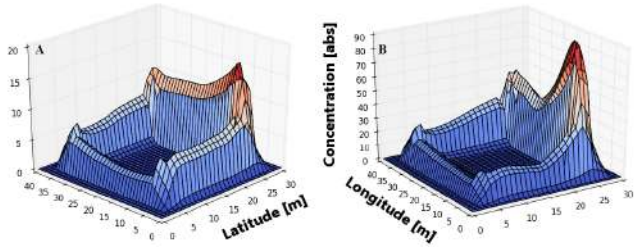

Fig. 2. Preliminary sensitivity test outdoor n.1, the MOX sensor was kept vertically above the gas sources 20 cm (case-A) and 10 cm (case-B) respectively.

periodic refill and maintenance of reagent substances. On the other hand, chemoresistive technology, also known as MOX sensors, offers fast response and long term stability without maintenance even if their power consumption is not negligible [18]. This permits the development of techniques for classification and fast detection such as the one proposed in [19]. To overcome the power consumption limit of MOXs, duty-cycle based strategies [20] or other low-power solutions [21], [22] have been demonstrated in literature which allow to greatly increase the lifetime of battery powered embedded electronic devices.

III. Chemicals Sensing

Metal-oxide sensors (MOX), typically used for static monitoring infrastructures and low-cost portable instruments, are essentially MOSFET transistors with a catalyst coated gate that interacts with gas vapors resulting in a modification of the gate charge and of the channel's conductive characteristics [12]. They do not provide an instantaneous measurement of the gas concentration, mainly because of the slow chemical interaction between metal and volatile compounds, moreover they require stable supply to precisely control the working temperature, as demonstrated for example in [23].

We used two off-the-shelf available sensors, namely, the MiCS-5121 [24] for CO/VOC and the MiCS-5525 [25] for CO measurement, both from SGX Sensortech Ltd[1]. The MiCS-5121 is a general CO/VOC sensor. This sensor and the mode of operation are designed to take measures of reducing gases such as carbon monoxide (CO), hydrocarbons (HC), and volatile organic compounds (VOC). The MiCS-5525 contains exactly the same sensitive element as the MiCS-5121 sensor, the only difference is the presence of a charcoal filter, which has been added on top of the sensitive element. Although we noticed that this charcoal filter increases the sensor reaction time and reduces the sensor sensitivity, conversely it enhances the selectivity.

The reversible chemical reaction they exploit is triggered by heat, to this reason they present the highest power consumption, with respect to any other surrounding electronic component on the measurement instrument. The main advantages of this family of sensors are the low-price, the lack of maintenance to refill chemical reagents and the lightweight, which is particularly of interest for application with flying

[1] http://www.sgxsensortech.com/

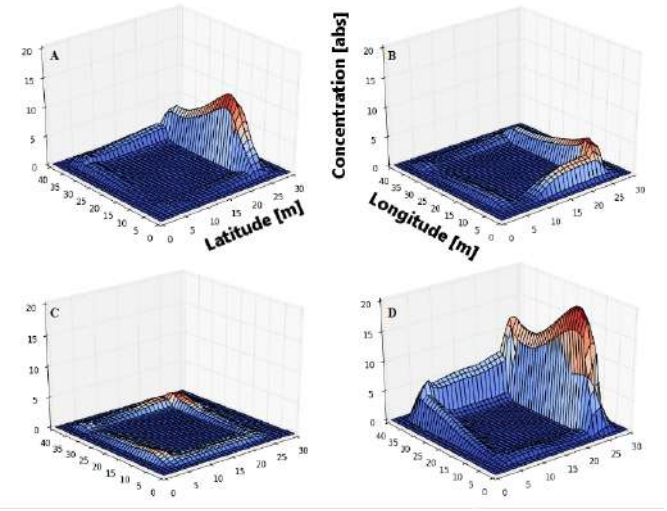

Fig. 3. Preliminary sensitivity test outdoor n.2, the MOX sensor was kept at different distances from the gas sources, 50 cm vertically (case-A), ≈ 70 cm diagonally (case-B), ≈ 110 cm diagonally (case-C) and 30 cm vertically (case-D).

carriers. Fig. 1 depicts the characteristic response of a MOX sensor used in this work, obtained in a controlled environment. After a warm up phase (stage-a), that is useful to assess the reference resistance in clean air condition, in presence of a gas leakage (in this case an open bottle of isopropyl alcohol) the sensor slowly reacts (stage-b) and the response stabilizes at a lower value within 5 s; finally, when the gas source is removed (stage-c), the sensor shows its long recovery time (≈ 50 s), that depends on the gas concentration and exposition time.

Although empirical, this analysis is useful to understand what happens in real cases since quantitative gas concentrations cannot be measured with only one sensor for two main reasons, (i) MOX sensors are characterized by a remarkable cross-sensitivity to family of chemical compounds and (ii) it's impossible to know a priori the composition of the volatile chemical scattered in the environment along with the target gas. Two main approaches exist to cope with these issues, (i) on one side it is possible to use an array of several sensors along with machine learning algorithms to discriminate both kind and concentration of chemicals [26]; (ii) otherwise a single sensor targeted to a family of compounds can be used as a trigger of a harmful situation and as a request for a specific analysis. The implication on size, cost and efforts required by the two approaches can be easily understood. In our application we selected the second option to reduce energy required, size and weight of the monitoring system prototype.

The gas distribution mapping and the localization of a static gas source are complex tasks, due to the turbulent nature of gas transport under natural conditions. Typically, turbulent transport is considerably faster compared to molecular diffusion. Apart from very small distances, where turbulence is not effective, molecular diffusion can be neglected concerning the spread of gas. A second important transport mechanism for gases, is advection due to prevailing fluid flow. Relatively constant air currents are typically found, even in an indoor environment without ventilation, as a result of pressure (draught) and temperature non-homogeneities (convection flow). Complexity increases considering outdoor environments where wind can play a major role in gas transportation in the atmosphere.

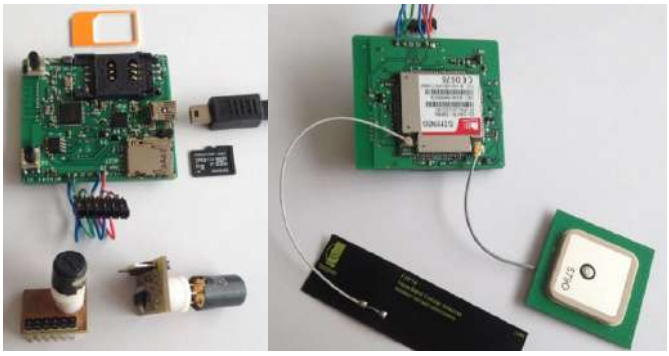

Fig. 4. The prototype 2-side readout board, on the left is shown the MCU and gas sensor side while on the right the combined GSM/GPS and antennas.

Considering the previous observation two tests on the field were carried out to evaluate the capability of MOX sensors to timely react with leakages in outdoor environments. These experiments were carried using the prototype acquisition board, equipped with the MiCS-5121 VOCs targeted sensor. We carried the system along a predefined rectangular path (20 m x 30 m long) where four gas sources were located at the corners: two bottles filled with different amount of acetone (coordinates 5:5 - latitude:longitude - for small amount of reagent and 25:5 for large quantity in the pictures) and two with different amount of isopropyl alcohol (coordinates 5:35 for the bottle with small amount and 25:35 for the large quantity in the pictures). The path was covered starting from position 0:0 toward location 5:5 and then following a counter-clockwise direction in all the experiments, with constant speed.

The first test aimed at verifying the sensor response in outdoor environment. Results shown in Fig. 2 illustrate the sensor response of two consecutive laps along the path with the sensing element vertically above the source and close approximately 20 cm during the first round (A) and 10 cm during the second (B), respectively. The reference concentration (flat area) represent the stable response of the sensor after the warm-up phase following the system switch-on. Obviously the shorter the distance the higher the response (notice the higher absolute value in picture 2-B), also with respect to the amount of reagent in the bottle. Moreover the long reaction and recovery time of sensor generates the wrong localization of the source that is particularly evident in case-B where the bottle of acetone located in position 25:5 results in a response spike in position 25:20.

In the second test, summarized in Fig. 3, we evaluated the sensitivity increasing the relative distance from sensor and sources. We started with the sensor 50 cm vertically above the bottle (case-A), then 50 cm both vertically and horizontally (≈ 70 cm of distance, case-B), 50 cm vertically and 100 cm horizontally apart from the bottles during the third round (case-C, ≈ 110 cm of distance) and the last lap was evaluated with 30 cm vertical distance from the bottles (case-D). Despite the low concentration of reagents (with respect to what we can

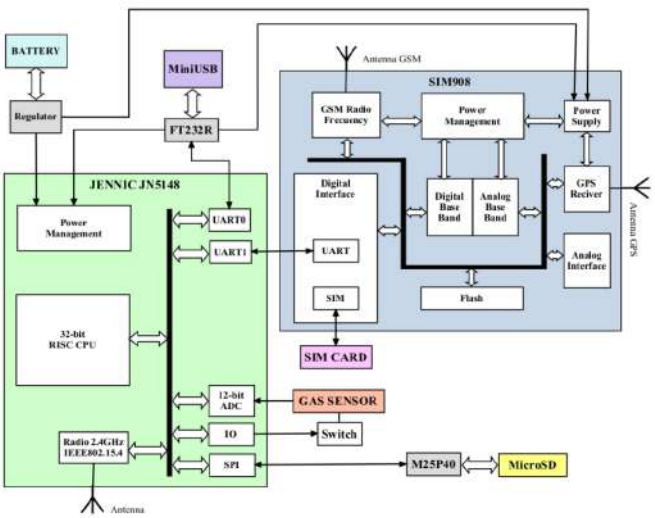

Fig. 5. Block scheme of the readout board with MCU, modem and external components.

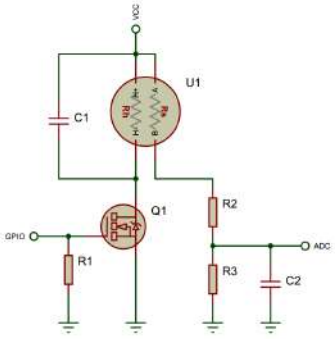

Fig. 6. Electrical scheme of the digitally controlled MOX sensors readout module.

expect from a pipe's leakage) the results show that the system is able to detect target volatile substances even without a forced convection device (pump or tube for active and passive convection, respectively).

Both tests were conducted outdoors, under moderate wind, variable environmental conditions (temperature, sun irradiance, humidity, etc.) and a non-constant aerial transportation and speed of propagation of volatiles. That results in fluctuations of the response, notice for example the difference (2 to 3 points in absolute value) between Fig. 2-B and 3-D. Both experiments demonstrate the capability of the system to detect and localize the region of the gas-leakages (characterized by a maximum) in a real environment, which is the major goal, while a quantitative measurement is marginal because it varies in the medium-long term.

IV. Embedded Platform

The architecture of the proposed mobile sensing system consists of two hardware units and antennas, sd-card and sim-card for a total occupancy of 4x4 cm and a weight less than 30 gr. (depicted in Fig. 4). The primary hardware unit hosts the MCU and the GSM/GPS modem and a bunch of auxiliary peripherals. The secondary unit is a gas sensor board designed

Fig. 7. Pictures of the UAV carrier (hexacopter with 80 cm diameter) and gas source taken during tests on the field.

to easily interface with the MCU. Both systems were designed by authors to optimize their use with mobile carriers.

A. Primary Unit

The MCU used is the JN5148[2] chip from NXP Company, which is a 32-bit microprocessor based on RISC design offering high performance and low power consumption. It integrates 128kB of ROM, 128kB of RAM, and a rich mix of analog and digital peripherals, such as the Serial Peripheral Interface (SPI), two independent Universal Asynchronous Receiver/Transmitter (UART) serial communication interfaces, TIMERs/COUNTERs, Analogue to Digital Converter (ADC) and others which allow to implement complex tasks. The MCU has also an integrated radio transceiver IEEE 802.15.4 compliant, designed for the implementation of Zigbee wireless networks. Although integrated, this radio interface exhibits high consumption and a short range of communication. We used it in test phase for real-time synchronization of the data with the base station, but we avoided to use it in the final algorithm to minimize energy consumption.

Implementation of tracking system requires receiving the GPS location, and the integration with GSM/GPRS modem, to be able to send or receive data. The current position of the object is provided by the SIM-908[3] integrated GSM/GPS transceiver, and then the data is sent via GPRS connection towards a dedicate web server with static IP, using TCP/IP protocol. The GPS engine is controlled by GSM engine, so when it is necessary to run GPS the GSM engine must be powered on and not in SLEEP mode.

The power unit consists of a rechargeable, 3.6 V, 1800 mAh, Lithium-ion battery, from a Nokia N73 smartphone. Fig. 5 depicts the mobile gas sensing system's block scheme and the connections between modules.

B. Secondary Unit

The small secondary unit has been designed to easily interface the gas sensor with the MCU using four lines, two for the supply, one digital enable signal and the analog output

[2]http://www.jennic.com/products/wireless_microcontrollers/
[3]http://www.simcom.us/product_detail.php?cid=1&pid=38

from the sensor. We realized a dedicated printed circuit board (PCB - shown in Fig. 4-left), to host the necessary signal conditioning circuit. Fig. 6 shows its design where `GPIO` stands for the digital enabling line, `ADC` is the analog output signal and finally `VCC` is a 3 V line form the regulated supply of the MCU. Alternatively, it could be possible to use one Digital to Analog (DAC) converter module of the MCU to provide modulated supply to the sensing element, if required; which is actually useless with the commercial devices considered in this work.

The sensing system developed for measuring gases include a single off-the-shelf available MOX sensor. This unit has been designed with standard socket for the sensing element to be interchangeable, to measure different gases and to fit the specific application. A stage of conditioning (`R2`, `R3` and `C2`) is required to adapt the analog signal of the MOX gas sensor to levels compatible with the ADC. Finally, the installation of a n-type MOSFET (`Q1`), used to switch the power signal on/off, keeps the power drained by the sensor under control. In this configuration, the MOX turns off at the same time as the device, saving power.

Both sensors are nominally driven at about 76 mW. The temperature rise of the heating resistor (R_h) is proportional to the applied power and the nominal working point is about 340° C. The gas measurement is taken by sampling the sensing resistance (R_s) which variation is inversely proportional to the volatile concentration, the higher the concentration, the higher the number of charge carriers, the lower the resistance. The operating range of chemoresistive sensors is quite high (from few MΩ to tens of kΩ), thus a high resolution ADC module is required to measure both supply voltage and sensor response. We used the 12-bit ADC integrated in the MCU. Thanks to the inverse relationship between V and R; and the voltage divider readout circuit, we obtained a non-linear resolution in the two decade range under evaluation. By carefully dimensioning the components (`R2`=2.2kΩ, `R3`=6.8kΩ, `Vcc`=3.2V) and the ADC reference (`Vref_adc`=1.6V) we achieved an adequate resolution for the application scenario. For example, we get ≈20kΩ resolution when the sensor's response is in the 1MΩ range, 300Ω @ 100kΩ down to 6Ω @ 10kΩ. In all the cases we get a resolution of at least 2 orders of magnitude lower than the signal of interest (cfr. Fig. 1). The power drained by these devices is higher than any other peripheral in the module, as it is shown in Table I. This motivates the need of a careful optimization of the monitoring algorithm to maximize the autonomy of the complete module.

C. Field Tests

The purpose of the real field experiments were to evaluate the sensitivity of MOX sensors in presence of turbulent air flow generated by the drone's propellers and the placement of the embedded system that was fastened below the main body of the UAV, to have the sensing unit perpendicularly oriented with respect to the ground.

We run several experiments using a DJI hexacopter[4]; this drone is suitable for limited region gas distribution mapping thanks to its 80 cm diameter and 10 Ah battery capacity it assures 15 min autonomy with up to 2.5 kg maximum payload. The experiments took place in the surroundings of the University and Fondazione Bruno Kessler (FBK) buildings (the technological center in the city of Trento) using the MICS-5121 VOCs targeted sensor. Results of two experiments are summarized using a map shown in Fig. 8. In the first one we tested the system's sensitivity during the flight with isopropyl alcohol (Fig. 7). In the second experiment the UAV surveyed the kitchens of the FBK center (smaller spot in the rectangle

[4]http://www.dji.com/product/spreading-wings-s800/feature

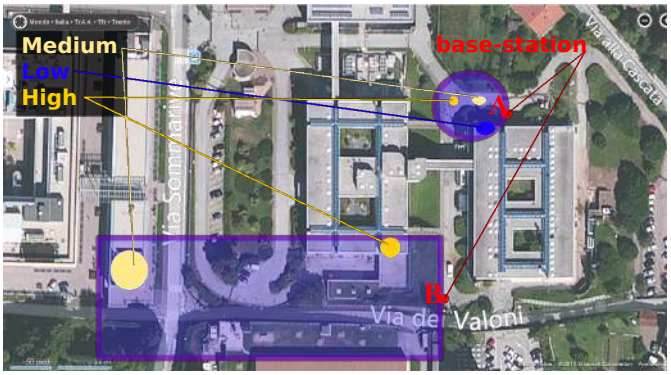

Fig. 8. Summary of the field tests with hexacopter. Superposition of the measured gas distribution map and aerial view of the test location.

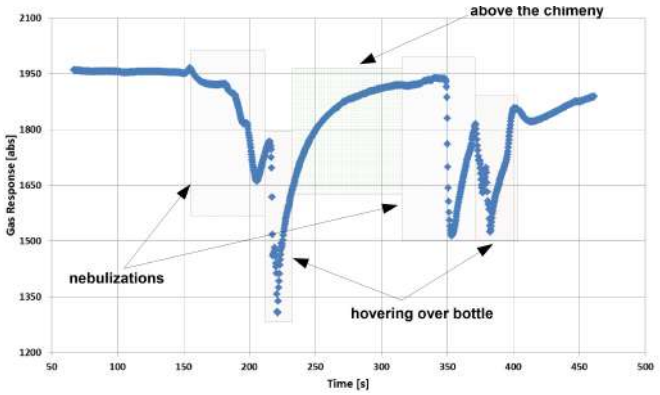

Fig. 9. Detailed results from the first flight test with hexacopter carrying the gas mapping instrumentation.

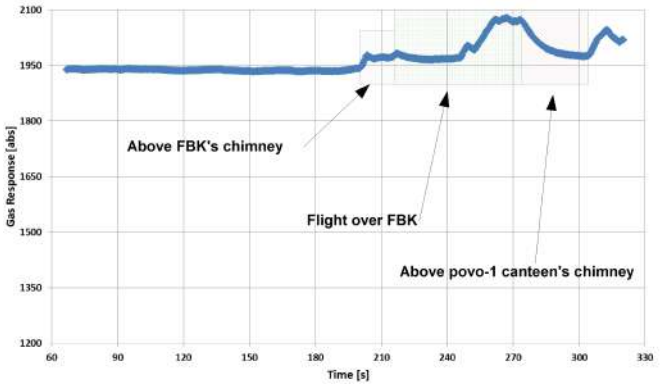

Fig. 10. Detailed results from the second flight test with hexacopter carrying the gas mapping instrumentation.

TABLE I
AVERAGE CURRENT CONSUMPTION REQUIRED BY THE OPERATING MODES, COMPUTED USING 1 Ω SHUNT RESISTOR.

Status			Consumption
MCU	**GPS/GSM**	**MOX**	**[mA]**
sleep	off	off	<1
on	off	off	12.50
on	off	on	51.25
on	on	off	33.75
on	on	on	75.00
on (LogSD)	off	off	35.60
on (LogSD)	on	off	56.25

of Fig. 8 marked with high concentration) and the University canteen (bigger spot in the same rectangle).

Detailed responses are reported in Figures 9 and 10. In both pictures, the decreasing spikes highlight the sensitivity of the system to react to volatile substances in air (marked with arrows and boxes). The second experiment, that covered a wider spatial range, demonstrates the capability of the system to react to changes in the environment, the increase in the response can be noticed when the drone is in between the two buildings (less VOCs concentrations can be assumed) while a decrease occurs just on top of the University canteen's chimneys that demonstrates the gas sources localization during movements.

These results confirms that environmental conditions and cross correlation of volatile chemicals strongly affect MOX's response, moreover the characterization of these responses in open environments is a challenging task, to this reason we want to move to multiparametric custom MOX sensors to eventually achieve volatile discrimination. Moreover the measurement unit's placement has demonstrated good enough from the sensitivity point of view, in this respect we observed the air flow generated by propellers does not blow away the volatile compounds spread in air and it was decide not to use any auxiliary convection equipment also in this configuration.

In these experiments, the prototype unit demonstrated ≈30 min autonomy of continuous gas sampling, data logging and wireless data streaming, which is longer than the autonomy of the employed UAV. We expect to further increase the energy autonomy by introducing improved sampling strategies based on duty-cycled sensor usage and aggressive data compression using compressive sensing techniques [27], [28].

V. ENERGY OPTIMIZATION

The definition of the monitoring strategy to optimize the lifetime of the mobile sensing system has been carried out using a simulating framework developed ad hoc, in Matlab environment, considering an Unmanned Aerial Vehicle (UAV) as carrier. This framework has been designed using generic models (except for the gas monitoring prototype) to be modular, customizable and ready for improvements. We firstly defined the monitoring strategy for the sensing module, then we characterized behavior and performance of each single stage of the system during monitoring to finally build a detailed model of execution time and energy requirements. We simulated the UAV considering a set of constant-speed experiments along straight paths. This simplistic approach perfectly fits leakage detection tasks for example in outdoor pipes monitoring. In the following, firstly the details of the monitoring strategy and model of the mobile sensing system are provided; secondly the energy optimization algorithm for chemical concentration measurement is presented.

TABLE II
MEASURED TIME REQUIRED BY THE SINGLE SAMPLING STAGES

Task	**Time [ms]**
LogSD	150
ADC Measure	1026
GPS request	5125
Mean Measure	5
Total	**6805**

A. Model Development

We developed the model of the mobile sensing system by characterizing the execution of the embedded application. This is based on a finite state machine where firstly the MCU and the GPS/GSM module are initialized, along with other peripherals like the ADC and the SD-card controller for logging. Then the main loop is started, here the gas measurement are collected and time-stamped with the GPS provided information (UTC time and coordinates). Gas measurement occurs for 1 s with a fixed rate of 500 μs per sample, for a total of 2000 $samples$. The heating time of 1 s is considered sufficient for MOX devices when the duty-cycle is higher than $\approx 1\%$ (e.g. 1 s against 1 min sleep-time), to ensure the quality of service and fast response. We have chosen this standard routine based on the results of several experiments not reported for the sake of summary and based on the observation in [20]. In the end the mobile system is set to sleep-mode depending on the duty-cycle which is defined by the optimization algorithm. We also included an Alert System to prevent risks and damages to people or property a routine that sends text messages to a predefined mobile phone. Although, we didn't modeled this sub-routine for the evaluation of the optimization algorithm. It consists on a plain text message containing relevant information about the system, such as the vehicle location and gas concentration. In addition, the system is also able to notify the user of other potential risks, like low battery.

The model used in the simulating framework is based on the sum of the energy required by each state, computed as the product of time and average power (considering the reference voltage). Notice that the current required by the sleep-mode is less than 1 mA (in the order of few hundreds of μA) so it is possible to neglect this contribution in the sum. Tables I and II present the mean values used to compute the model, obtained by averaging a dozen of experiments. In this characterization we used a custom rechargeable battery pack made of 3, AA-type batteries connected in series (1.5 V, 2500mAh each).

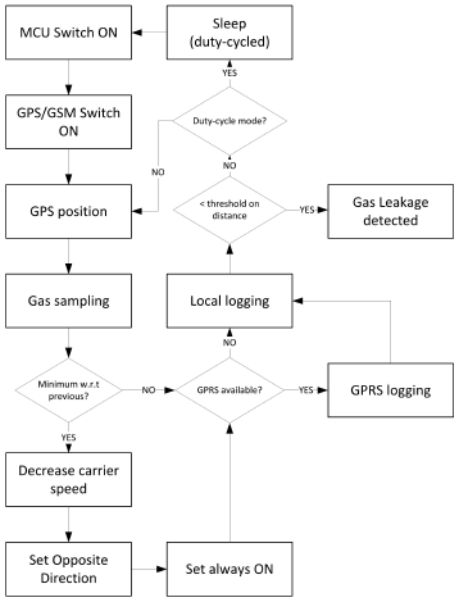

Fig. 11. Block scheme of the tracking algorithm based on the hill-climbing approach.

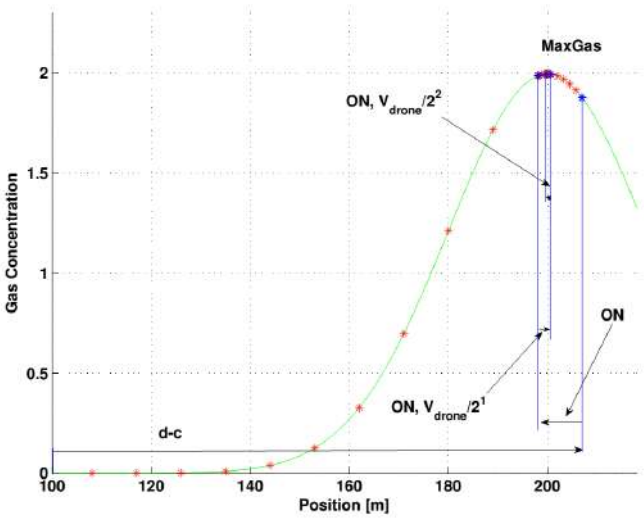

Fig. 12. Graphical representation of the system evolution (monitoring instrument and carrier) during the optimization routine.

The current has been measured using 1Ω shunt resistor in series with the negative supply pole, while the time has been measured using an oscilloscope[5]. If the system works continuously in ON state, with a mean consumption of 75 mA, it lasts for 1 day and 9 hours approximately. Which is longer than the expected UAV autonomy (for commercial devices). The main tuning parameter, that is the optimization target, is the duty-cycle (dc subscript in the following pictures) defined as the overall ON-time, regardless of the state, divided by the total time (ON-time and sleep-interval).

[5]Agilent DSO7032A Oscilloscope http://www.keysight.com/en/pd-1293547-pn-DSO7032A/oscilloscope-350-mhz-2-channels

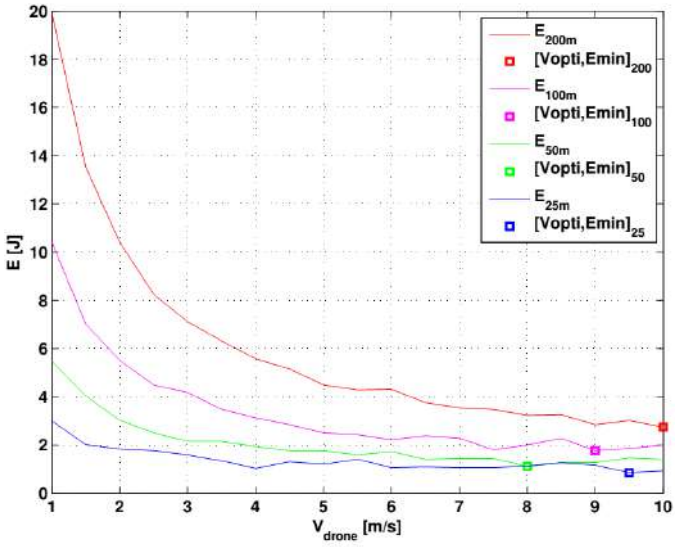

Fig. 13. Results of the simulations in terms of optimal carrier speed against mobile system energy consumption and gas leakage locations.

B. Algorithm

Here we describe the gas source location strategy that optimizes the speed of the robot while minimizing the monitoring system energy consumption. We implemented the mobile sensing system and UAV models in a discrete-time Matlab framework, considering a 2D representation of the environment where the UAV carrier moves. The first model has been presented above, while for the second one we used a linear motion equation. The shape of the gas distribution must be roughly circular with a strong central peak, being possible to use the maximum response peak of the gas sensor as an approximation of the gas source location. Previous studies conclude that the various theories of contaminants' distribution function tend to the Gaussian function. Thus we modeled the profile of gas concentration measures, using a 2D Gaussian distribution model. Fig. 12 shows the qualitative behavior of the algorithm, here the green line illustrates the 2D projection of the concentration along the path.

The searching is accomplished by applying a exploration strategy based on the "hill climbing" algorithm, summarized in the block scheme of Fig. 11. This strategy always converges to the optimal solution in the case of a single gas source. The optimal speed of the carrier is found after an exhaustive search of the state space determined by the set of initial carrier speeds (from 1 m/s up to 10 m/s) and duty-cycles. As described above the ON-time is fixed to ensure a reliable gas measurement, while the sleep-time was set as a parameter to compare the performance in different configurations (employed values are 11%, 20%, 33%, 50%, 55% and 71% duty-cycles). The gas leakage is placed at fixed distances from the carrier's starting position (reference 0 in the following) in the range from 25 m to 200 m.

The exploration algorithm operates by simulating the movements of the UAV carrier. Following the linear motion model, for every second the position is updated while the gas reading is updated according to the duty-cycle. Once the a new gas

sample is obtained it is compared with the previous. If it is greater or equal than the successor, then make it the current reference state called maximum (red points in Fig. 12). The algorithm continues until a decrease in the response is found. At this point the current state is marked as minimum (blue points in Fig. 12), the speed of the carrier is halved and the movement is oriented in the opposite direction. This process iterates until the distance between two successive minima is less than a fixed threshold (1 m). The loop is performed for all possible starting velocity of the carrier which decrease according to an exponential behavior described by the relation $V_{drone}^{next} = V_{drone}^{actual}/2^n$, where n is the iteration number, counting from 0 to N. For example, with a starting speed $V_{drone}^{start} = 10\ [m/s]$, if we assume to locate the gas leakage after 5 loops we get a final speed of $V_{drone}^{end} = 10/2^4 = 0.625\ [m/s]$. Finally the algorithm calculates the energy consumption to locate the gas leakage, and compares the energy spent for all speeds. Finally it returns the optimal speed that minimizes the energy consumption.

C. Simulated Results

A selection of results is presented in from Fig. 13 to 15. We can observe (Fig. 13) that the optimal speed is usually fast, which is intuitive, less time implies less consumed energy for the mobile sensing system. Moreover the optimal one depends on the distance from the gas source. Clearly when the distance to a gas source increases, the energy consumption increases as well. It is important to notice that the difference of consumed energy between high and low speeds decrease when the distance to a gas source decreases. Fig. 14 compares the duty-cycled strategy with a continuous monitoring approach, to underline its effectiveness especially at low speeds. Finally, Fig. 15 is useful to underline the remarkable difference between duty-cycles effects on current consumption which obviously require a careful evaluation. From these results we can conclude that the sampling resolution must be as quickly as possible to rapidly locate the area of interest and eventually to cope with the rapid dynamics intrinsic to gas propagation in real environments. However, to find the maximum with high accuracy, this speed must be reduced promptly, that is the reason for the exponential decrease adopted in the proposed approach.

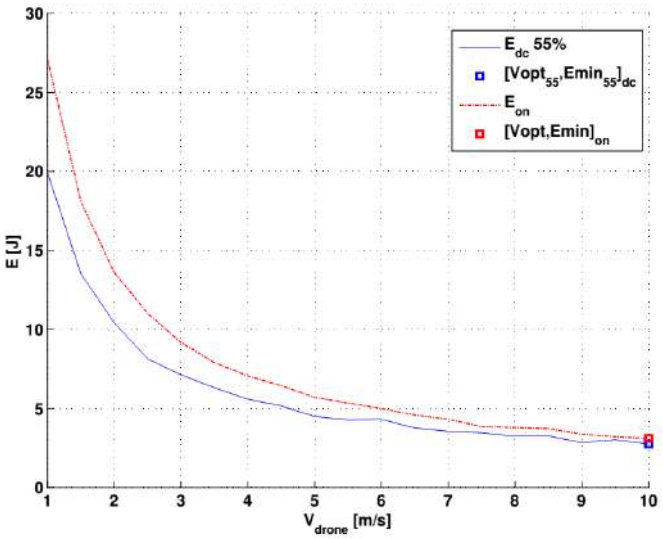

Fig. 14. Results of the simulations in terms of energy consumption of duty-cycled and continuous monitoring strategies as a function of the carrier speed.

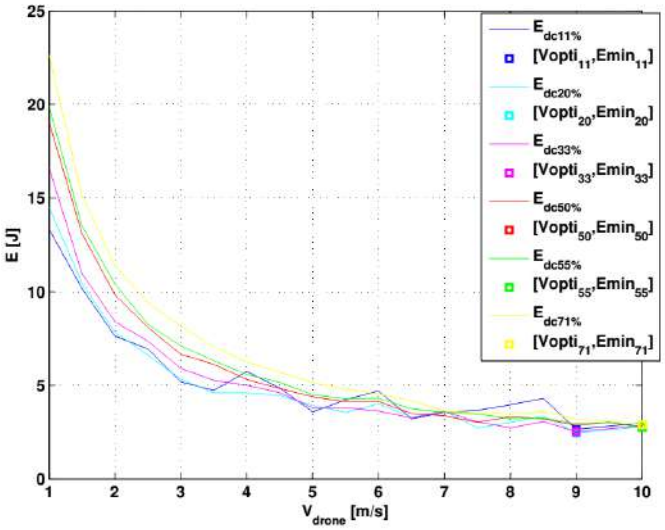

Fig. 15. Results of the simulations in terms of energy consumption of different duty-cycled monitoring approaches as a function of the carrier speed.

VI. Extending autonomy

In this last section we propose the design space exploration for the study of solar powered copter-like drones. This analysis is meant to evaluate the possible performance boost, in terms of extension of the flight autonomy, that could be achieved introducing solar energy harvesting capabilities in the drone carrier.

Copter-like UAVs, available in the market, have limited flight autonomy which severely limits their employment in wide-area unmanned monitoring applications. The main characteristics of a selection of commercial UAVs, provided by manufacturers, is presented in Table III for comparison, ranging from the toy-like Hubsan Nano Q4 up to the professional 3dr x8+ used by film-makers for stable aerial shooting. Maximum payload is the first parameter to consider in the choice of a carrier for custom monitoring applications, since it poses an upper bound to the size of the equipment that can be used without jeopardizing take-off capability and without reducing the flight autonomy below 50% of the nominal value.

By analyzing the information provided by manufacturers in data-sheets we computed the nominal power consumption of the copters (highlighted in the table) according to the following equation.

$$P_{[W]} = \frac{Capacity_{[C]}}{Autonomy_{[s]}} \cdot V_{BAT}$$

Those values are representative of nominal flying conditions (no wind, medium and constant speed) and account only for the drone's motion manually controlled using a remote without payload, no auto-pilot (using GPS) and no video streaming/recording (where available). Results demonstrate

TABLE III
COMPARISON OF MAIN FEATURES OF COMMERCIAL COPTER-LIKE DRONES

Copter Name	Weight [g]	Max Payload [g]	Voltage [V_{BAT}]	Capacity [mAh]	Autonomy [min]	Size [mm]	**Power Consumption [W]**
Hubsan nano q4	20	0	3.7	100	5	50x50	**4.44**
Crazyflie 2.0	27	15	3.7	240	7	92x92x29	**7.61**
DJI Phantom-2 v+	1242	800	11.1	5200	25	350 (d)	**138.53**
Hubsan x4 pro	1060	360	11.1	7000	30	370 (d)	**155.40**
Parrot ar.2.0 classic	400	$<$100	11.1	1000	12	570 (d)	**55.50**
3dr iris+	1282	400	11.1	5100	16	550 (d)	**212.29**
3dr x8+	2560	800	14.8	10000	15	350x510x200	**592.00**

TABLE IV
COMPARISON OF COMMERCIAL PHOTOVOLTAIC PANELS FEATURES

Panel Model	Power [W]	V_{OC} [V]	I_{SC} [mA]	V_{MPP} [V]	I_{MPP} [mA]	Size LxWxH [mm]	Weight [g]	Power/area [W/cm^2]
Traditional								
Multicomp MC-SP0.8-NF-GCS	0.8	4.8	2.30	3.85	210	140x100x4.9	134	0.0057
BP Solar MSX-005F	0.446	4.6	160	3.3	150	114.3x66.8x3	160	0.0006
BP Solar MSX-01F	1.2	10.3	160	7.5	150	127x127x3	340	0.0074
BP Solar SX-5M	4.5	20.5	300	16.5	270	245x269x22.6	800	0.0068
Solar Technology STP005BP	5	21	390	16.8	300	306x218x25	1000	0.0075
Solar Technology STP010BP	10	21	660	16.8	590	397x280x25	1500	0.0090
ThinFilm								
PowerFilm MP7.2-150	1.44	10.5	150	7.2	220	253x146x0.61	25.9	0.0039
PowerFilm MPT15-150	1.54	19	120	15.4	110	253x146x0.61	26	0.0042

that power consumption is remarkably high even for the very small copters.

Considering the negligible payload introduced by the proposed gas sensing equipment with respect to the nominal weight of the drones (excluding the first two in the list), we propose to extend the flight autonomy with the method already demonstrated with airplane-like drones, namely including photovoltaic panels in the structure of the copter to harvest solar energy during the flight, as shown in the concept depicted in Fig. 16, where a polycristalline pv panel has been stuck between body and propellers of a Crazyflie 2.0 micro-drone (with no gas sensing board).

Drones can fly only in clear sky conditions with low wind intensity, due to strict safety regulations promoted in the last years. Optimal conditions also for PV panels to achieve the maximum power production with good solar energy harvesters [29]. Several questions arise in this context, for example, how can we modify the shape of the copter to host one or more panels? Which is the best orientation to maximize the conversion efficiency in any displacement? And what is the impact on the payload of the energy conditioning circuitry? Should we add another accumulator or not? According to our point of view, the first thing to evaluate is the impact on the autonomy that can be achieved. In other words, how long the flight-time can be extended. To address this issue, we analyzed several PV panels available on the market with the aim to select suitable components for the evaluation. Table IV lists few commercial devices that are arranged in two groups, traditional and thin film (bendable). Numbers show that thin film panels are extremely lightweight and could be a good candidate for the UAV's upgrade, however their efficiency (expressed here as power to size ratio) it is slightly more than half of the traditional ones.

Table V presents the ration between the runtime power consumption and the expected power contribution from the PV harvester. It indicates the percentage of power which can be extracted during the flight from the environment, using PV panels with 0.0074 W/cm^2 efficiency (as for MSX-01F panels) on the available surface of the drone. This method contributes to the overall power budget and allows to extend the flight autonomy correspondingly. Results show that, using drones that could carry the weight of such structure, the maximum achievable gain is less than 6% which means longer flight autonomy as reported in the last column of the table. Only the lightweight Parrot AR 2.0 Drone could significantly boost its autonomy up to 20%.

TABLE V
EXPECTED PV PANELS PERFORMANCE GAIN

Copter Name	Area [cm^2]	PV Power [W]	PV/P [%]	Gain [s]
DJI Phantom-2 v+	612.50	4.56	3.29	49
Hubsan x4 pro	684.50	5.09	3.28	59
Parrot ar.2.0 classic	1624.50	12.09	**21.78**	**157**
3dr iris+	1512.50	11.25	5.30	51
3dr x8+	1785.00	13.28	2.24	20

Fig. 16. Experiment of a solar powered drone using a CrazyFlie 2.0 and a 70x55 mm solar panel.

VII. CONCLUSION

In this work we present the design and characterization of an embedded platform meant for gas distribution mapping and leakage localization applications using Unmanned Aerial Vehicles as mobile carrier. Main features of the measurement instrument are the low-power consumption and the small form-factor, achieving long autonomy on its own rechargeable battery. Field experiments demonstrate the sensitivity of the measurement instrument equipped with VOC targeted MOX sensors both in stand-alone and mounted as a payload of an UAV.

To fulfill the low-power design of the complete mobile system and maximize the currently limited flight autonomy we developed an optimal monitoring algorithm to autonomously drive the carrier based on the feedback from the gas measurement unit and evaluated the boost in performance that can be achieved by introducing a photovoltaic harvesting unit directly on-board.

REFERENCES

[1] V. Gallego, M. Rossi, and D. Brunelli, "Unmanned aerial gas leakage localization and mapping using microdrones," in *Sensors Applications Symposium (SAS)*. IEEE, Apr 2015.

[2] M. Rossi, D. Brunelli, A. Adami, L. Lorenzelli, F. Menna, and F. Remondino, "Gas-drone: Portable gas sensing system on uavs for gas leakage localization," in *SENSORS, 2014 IEEE*, Nov 2014, pp. 1431–1434.

[3] J. K. Hart and K. Martinez, "Environmental sensor networks: A revolution in the earth system science?" *Earth-Science Reviews*, vol. 78, no. 3, pp. 177–191, 2006.

[4] E. Santamaria, F. Segor, I. Tchouchenkov, and R. Schoenbein, "Rapid aerial mapping with multiple heterogeneous unmanned vehicles," *International Journal On Advances in Systems and Measurements*, vol. 6, no. 3 and 4, pp. 384–393, 2013.

[5] F. Nex and F. Remondino, "Uav for 3d mapping applications: a review," *Applied Geomatics*, vol. 6, no. 1, pp. 1–15, 2014.

[6] P. P. Neumann, S. Asadi, A. J. Lilienthal, M. Bartholmai, and J. H. Schiller, "Autonomous gas-sensitive microdrone: wind vector estimation and gas distribution mapping," *Robotics & Automation Magazine, IEEE*, vol. 19, no. 1, pp. 50–61, 2012.

[7] D. Caltabiano, G. Muscato, A. Orlando, C. Federico, G. Giudice, and S. Guerrieri, "Architecture of a uav for volcanic gas sampling," in *Emerging Technologies and Factory Automation, 2005. ETFA 2005. 10th IEEE Conference on*, vol. 1. IEEE, 2005, pp. 744–749.

[8] K. Daniel, B. Dusza, A. Lewandowski, and C. Wietfeld, "Airshield: A system-of-systems muav remote sensing architecture for disaster response," in *Systems Conference, 2009 3rd Annual IEEE*. IEEE, 2009, pp. 196–200.

[9] J. Allred, A. B. Hasan, S. Panichsakul, W. Pisano, P. Gray, J. Huang, R. Han, D. Lawrence, and K. Mohseni, "Sensorflock: an airborne wireless sensor network of micro-air vehicles," in *Proceedings of the 5th international conference on Embedded networked sensor systems*. ACM, 2007, pp. 117–129.

[10] A. Purohit, Z. Sun, F. Mokaya, and P. Zhang, "Sensorfly: Controlled-mobile sensing platform for indoor emergency response applications," in *Information Processing in Sensor Networks (IPSN), 2011 10th International Conference on*. IEEE, 2011, pp. 223–234.

[11] A. Malaver, N. Motta, P. Corke, and F. Gonzalez, "Development and integration of a solar powered unmanned aerial vehicle and a wireless sensor network to monitor greenhouse gases," *Sensors*, vol. 15, no. 2, pp. 4072–4096, 2015.

[12] H. Nagle, R. Gutierrez-Osuna, and S. Schiffman, "The how and why of electronic noses," *Spectrum, IEEE*, vol. 35, no. 9, pp. 22–31, Sep 1998.

[13] M. Rossi and D. Brunelli, "Ultra low power ch4 monitoring with wireless sensors," in *SENSORS, 2013 IEEE*, Nov 2013, pp. 1–4.

[14] S. So, F. Koushanfar, A. Kosterev, and F. Tittel, "Laserspecks:: laser spectroscopic trace-gas sensor networks-sensor integration and applications," in *Proceedings of the 6th international conference on Information processing in sensor networks*. ACM, 2007, pp. 226–235.

[15] M. Rossi and D. Brunelli, "Analyzing the transient response of mox gas sensors to improve the lifetime of distributed sensing systems," in *Advances in Sensors and Interfaces (IWASI), 2013 5th IEEE International Workshop on*, June 2013, pp. 211–216.

[16] D. Brunelli and M. Rossi, "Enhancing lifetime of wsn for natural gas leakages detection," *Microelectronics Journal*, vol. 45, no. 12, pp. 1665–1670, 2014.

[17] D. Wang, D. P. Agrawal, W. Toruksa, C. Chaiwatpongsakorn, M. Lu, and T. C. Keener, "Monitoring ambient air quality with carbon monoxide sensor-based wireless network," *Communications of the ACM*, vol. 53, no. 5, pp. 138–141, 2010.

[18] J. Yu, J. Li, Q. Dai, D. Li, X. Ma, and Y. Lv, "Temperature compensation and data fusion based on a multifunctional gas detector," *Instrumentation and Measurement, IEEE Transactions on*, vol. 64, no. 1, pp. 204–211, Jan 2015.

[19] A. Ozmen and E. Dogan, "Design of a portable e-nose instrument for gas classifications," *Instrumentation and Measurement, IEEE Transactions on*, vol. 58, no. 10, pp. 3609–3618, Oct 2009.

[20] M. Rossi and D. Brunelli, "Ultra low power mox sensor reading for natural gas wireless monitoring," *Sensors Journal, IEEE*, vol. in press, 2014.

[21] L. Bissi, M. Cicioni, P. Placidi, S. Zampolli, I. Elmi, and A. Scorzoni, "A programmable interface circuit for an ultralow power gas sensor," *Instrumentation and Measurement, IEEE Transactions on*, vol. 60, no. 1, pp. 282–289, Jan 2011.

[22] M. Rossi and D. Brunelli, "Ultra low power wireless gas sensor network for environmental monitoring applications," in *Environmental Energy and Structural Monitoring Systems (EESMS), 2012 IEEE Workshop on*, Sept 2012, pp. 75–81.

[23] A. Depari, A. Flammini, D. Marioli, E. Sisinni, E. Comini, and A. Ponzoni, "An electronic system to heat mox sensors with synchronized and programmable thermal profiles," *Instrumentation and Measurement, IEEE Transactions on*, vol. 61, no. 9, pp. 2374–2383, Sept 2012.

[24] "MICS-5121 data sheet," SGX Sensortech Limited. [Online]. Available: http://www.cdiweb.com/datasheets/e2v/a1a-mics-5121_2_v1.pdf

[25] "MICS-5525 data sheet," SGX Sensortech Limited. [Online]. Available: http://www.cdiweb.com/datasheets/e2v/mics-5525.pdf

[26] K. Brudzewski, S. Osowski, and A. Dwulit, "Recognition of coffee using differential electronic nose," *Instrumentation and Measurement, IEEE Transactions on*, vol. 61, no. 6, pp. 1803–1810, June 2012.

[27] D. Brunelli and C. Caione, "Sparse recovery optimization in wireless sensor networks with a sub-nyquist sampling rate," *Sensors*, vol. 15, no. 7, p. 16654, 2015.

[28] B. Milosevic, C. Caione, E. Farella, D. Brunelli, and L. Benini, "Sub-sampling framework comparison for low-power data gathering: A comparative analysis," *Sensors*, vol. 15, no. 3, p. 5058, 2015.

[29] D. Carli, D. Brunelli, L. Benini, and M. Ruggeri, "An effective multi-source energy harvester for low power applications," in *Design, Automation Test in Europe Conference Exhibition (DATE), 2011*, March 2011, pp. 1–6.